Study of Packaging and Installation of FBG Sensors for Monitoring of Aircraft Systems

Study of packaging and installation of FBG sensors for monitoring of aircraft systems

Pier Carlo Berri
Dept.of Mechanical & Aerospace Engineering, Politecnico di Torino, Italy. E-mail: pier.berri@polito.it

Cosimo Corsi
Dept.of Mechanical & Aerospace Engineering, Politecnico di Torino, Italy. E-mail: cosimocorsi94@gmail.com

Matteo D.L. Dalla Vedova
Dept.of Mechanical & Aerospace Engineering, Politecnico di Torino, Italy. E-mail: matteo.dallavedova@polito.it

Alessio D. Laudani
Dept.of Mechanical & Aerospace Engineering, Politecnico di Torino, Italy. E-mail: alessio.laudani4@gmail.com

Paolo Maggiore
Dept.of Mechanical & Aerospace Engineering, Politecnico di Torino, Italy. E-mail: paolo.maggiore@polito.it

Cristian Secci
Dept.of Mechanical & Aerospace Engineering, Politecnico di Torino, Italy. E-mail: cristiansecci@gmail.com

Next generation aircraft systems will feature an ever increasing complexity. In this context, advanced health monitoring strategies will be required to ensure a high level of operations safety as well as a good reliability. Hence, Prognostics and Health Management (PHM) is emerging as an enabling discipline for future advanced aircraft design and operations, with a particular application to Flight Control System (FCS) monitoring.
One of the most critical issues for real-time Fault Detection and Identification (FDI) of aircraft FCS is the availability of actuator load measurements. The aerodynamic load on flight control actuators has a significant influence on their dynamic response, and can easily hide the effect of incipient failure precursors. For this reason, real-time monitoring FDI algorithms relying on the comparison between the actual system response and that of a digital twin require either a measure or an estimation of aerodynamic loads.
Usually, this quantity is not monitored by a dedicated sensor, since it is not required as a feedback signal by most control logics. A dedicated load sensor for PHM with traditional technologies is not easily feasible: for example, a load cell would be mechanically connected in series with the actuator, adding a potential single failure point and affecting the overall system safety; the use of strain gages on the structure is less accurate, and requires several sensors with individual wiring and complex signal conditioning circuitry. Optical strain sensors based on Fiber Bragg Gratings (FBG) allow indirect load measurement combined with real-time structural monitoring, combining an acceptable increase in complexity and costs with a high robustness.
In this preliminary study, we installed an FBG monitoring system on a UAV to assess the feasibility of such technology. Measures of structure deflection were correlated to actuator position and IMU data, to estimate aerodynamic loads.

Keywords: Structural Health Monitoring, FBG sensors, Prognostics, Flight Control system, Flight test

1. Introduction

Fault Detection and Isolation (FDI) algorithms for prognostics of aircraft systems are required to identify the early failure precursors, when their effect on system performances is still small or negligible. For this reason, a large quantity of data and measures of the system working parameters need to be analyzed; the sensors used to measure those data are required to be very accurate, in order to avoid the sensor noise to hide useful information on the components health.
Common FDI approaches for aircraft Flight Control System (FCS) leverage either machine learning algorithms, as highlighted by Anderson and Aylward (1993), De Martin et al. (2019) or a model based strategy, as proposed by Dalla Vedova et al. (2019), Hasan and Johansen (2018), or a combination of the two , as proposed by Berri et al. (2018, 2019a). Model-Based FDI compares the response of the system with that of a digital twin. However, the response of a flight control actuator is greatly influenced by both the command and load signal.

The former is obviously known, but the latter is not usually available, and then cannot be accounted for in the simulation of the digital twin. As a consequence, to perform successful real-time FDI of flight control actuators, a measure of the aerodynamic load is required.
Different technologies are possible to measure the actuator load. A direct measure performed through a load cell gives accurate evaluation of the force, but, being the cell connected in series to the actuator itself, a single-failure point is added to the system, decreasing the overall safety. An alternative is the placement of strain gages on the airframe structure, in proximity of the actuator connection points. This technique is less invasive, but inherently more complex, since data from several sensors must be combined to filter out the effects of external forces influencing the reading (e.g. rigid-body accelerations, lift distribution, external payloads, etc.) Willcox and Mainini (2017a, 2017b). Additionally, traditional resistive strain gages require individual wiring and signal conditioning circuitry, and the system complexity can grow to unacceptable levels.
An alternative solution allowing the installation of a distributed strain sensors network to determine flight control actuators loads involve employing of Fiber Bragg Grating (FBG) optical sensors, described by Mihailov (2012). Those consist in a small section of an optical fiber, treated to be sensitive to deformation, either mechanical or thermal. The FBG-based sensors can be used as a replacement of traditional strain gages in many applications. They provide strain measures of comparable accuracy, but are totally insensitive to electromagnetic interference and are compatible with hostile environments Mihailov et al. (2017). As highlighted by Santos and Farahi (2018), a single optical fiber can handle tens to hundreds of sensors: then a distributed measure can be achieved avoiding the issues related with individual wiring and signal conditioning circuitry of strain gages.
Conversely, as shown by Tanaka et al. (2003), as FBGs are highly sensitive to temperature, thermal compensation must be quite accurate, and the small surface area of the sensors require a careful gluing to ensure mechanical continuity and a rigid connection with the structure, for proper load transfer. In this work we present an experimental campaign aimed at validating the use of FBG sensors for actuator load estimation and structural health monitoring. The sensors have been installed on a UAV platform and tested in-flight to determine the performance of the system. A deeper study for data post processing and real-time actuator load reconstruction under development, will be presented in a future work.

2. Experimental setup

We tested an FBG based Structural Health Monitoring system on a radio controlled UAV. The aircraft (represented in Figure 1) was provided by the ICARUS PoliTO students team, and is a competition motor glider of 11.9kg MTOW and 4m wingspan.

Fig. 1. Render of the UAV employed for flight tests.

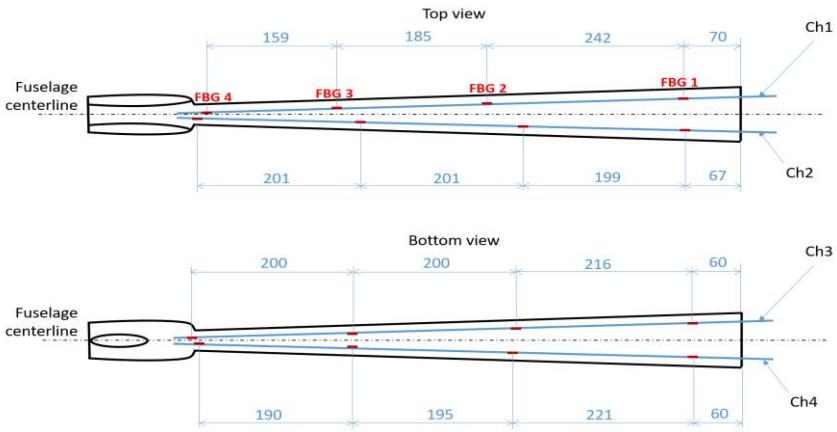

Fig. 2. Positioning of the FBGs on the tail beam (a)

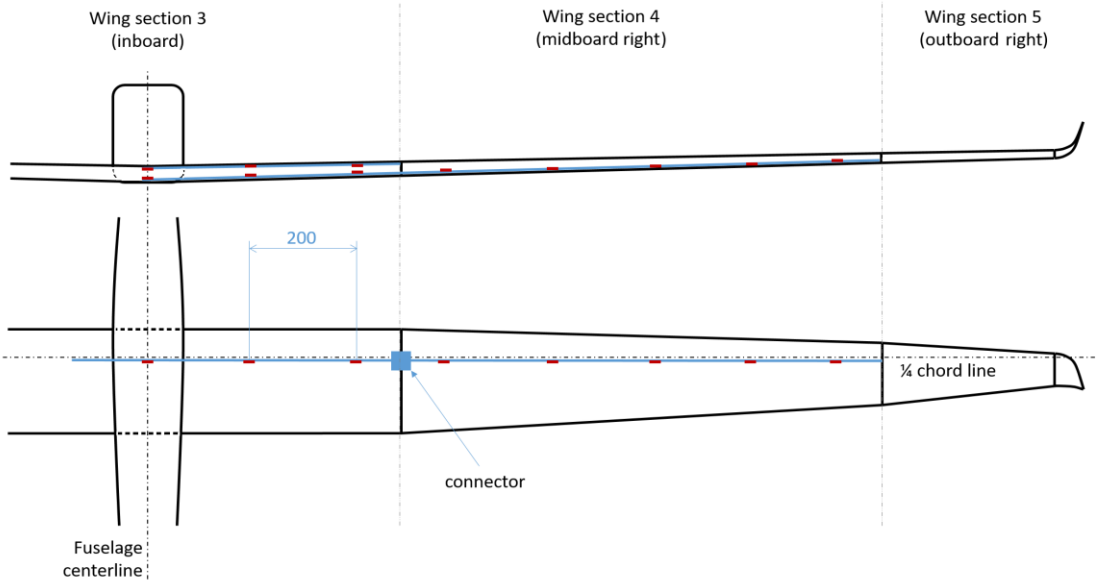

Fig. 3. Positioning of the FBGs on the inboard and mid wing sections

It was designed for an 8kg payload, for participating to the 2017 edition of the Aircraft Cargo Challenge organized by the University of Zagreb. The platform features a composite (CFRP) modular structure and a payload capability compatible with the installation of the system. A preliminary assessment of the material characteristics was carried out through a campaign of tensile and flexural tests. The system consisted in a SmartScan interrogator reading the measures of a network of sensors installed on the UAV wing and tail beam. Data was transmitted by the interrogator via an Ethernet protocol and logged on a SD card by a Raspberry Pi.

2.1 *Placement of sensors*

We decided to install sensors on the tail beam (for ease of installation) and on two wing section. A total of 16 sensors in 4 channels were installed on the tail, and 11 sensors in 2 channels on a wing spar (3 between the upper spar cap and skin and 8 between the lower spar cap and skin). The installation of 5 additional sensors on the upper spar cap war planned, but an issue during the manufacturing process prevented the connection of the related channel. All sensors were glued to structural components with epoxy resin, as this was shown by Berri et al (2019b) to result in good accuracy of the measures.

Figure 2 shows the placement of the 16 FBG sensors on the tail beam. Four traditional Strain Gages (SGs) were installed close to the FBGs of channel 1, in order to compare and validate the measures of the optical sensors during the static tests. The SGs were wired only temporarily for the static tests, and were not intended to be used in flight, as their signal conditioning and acquisition circuitry is large and would not fit into the payload bay of the UAV. The location of the 11 sensors installed on the wing is represented in Figure 3. The wing is divided into five sections. All the wing FBGs are equally spaced with a 200mm pitch, starting from the aircraft centerline. The modular construction of the wing requires to adopt a disassemblable solution for the sensors; this is achieved by introducing an optical connector between two adjacent wing sections. FBGs were installed on section 3 (inboard section and wing-fuselage connection) and 4 (right mid section). Section 5 (right outboard section) was not considered for sensor installation, since it is lightly loaded and accounts for a small fraction of the total span. Additionally, installation of sensors on section 5 would have required the addition of two connectors on the optical line, introducing an optical loss, increasing the complexity, and degrading the performance and reliability of the system.

2.2 *Power and weight budget for the Optical Structural Health Monitoring system*

The overall system installed on the UAV includes the FBG sensors, interrogator, Raspberry Pi, and dedicated batteries. The interrogator needs an average current of 1.0A@9-36V power supply.

Table 1. Weight breakdown of the Optical Structural Health Monitoring system

Component	Weight (g)
SmartScan FBG interrogator	1100
Raspberry Pi	45
Interrogator Battery	419
USB power bank	360
FBG sensors	<1
Wiring and connectors	30
Total	**1955**

This is achieved with a 6000mAh, 3S LiPo (11.1V), theoretically able to provide an endurance of 6 hours, much longer than the max flight endurance of the aircraft. The reason for such oversizing of the battery is twofold: the battery acts as a ballast to get the center of gravity back within the acceptable range, since the installation of the interrogator results in an excessive pitch up attitude; additionally, the battery that was employed is equal to that of the powerplant and was already available as a spare. The oversized endurance also avoids to damage the battery itself for excessive discharge, since the interrogator is not fitted with a battery protection circuit. The Raspberry Pi was powered with a 20000mAh USB power bank; for future flight tests, we plan to replace the power bank with a DC-DC converter, to use a common battery for the interrogator and Raspberry, and achieve a weight reduction in the order of 300g. The weight of sensors is negligible with respect to the other components, and the total weight of the system is 1955g, well within the maximum design payload of the UAV platform. As appears from the weight breakdown of Table 1, a large fraction of the system weight is due to the oversized battery employed. The system is easily scalable as several sensors can be stacked on the same optical fiber. The weight of the sensored fiber is negligible (in the order of 30g to 50g per kilometer), and the acquisition system, while significant on the weight budget of a small UAV, is not demanding in terms of weight, nor in terms of required power, for the installation on a full scale aircraft. The sensors for both the wing and tail were calibrated with a static load test at first, which allowed to assess the correct operation of the system. Data acquired under actual flight loads allowed to determine the signal quality, the noise, caused by mechanical vibration and aerodynamic turbulence, as well as the invasivity and scalability of the system at aircraft level.

3. Static tests results and sensors calibration

A preliminary assessment of the material characteristics was carried out with a campaign of axial strain and flexural tests on rectangular samples of the same CFRP as that employed for. the aircraft structure.

A first assessment of the accuracy of the sensors was performed through a static load test, for both the wing and fuselage. The readings from FBGs were compared with FEM simulations and traditional strain gages. The SGs allowed to calibrate the Finite Elements model to the actual characteristics of the employed material (which, due to uncertainties in the control of the production process, were not accurately known, even after the preliminary tensile and flexural tests). The FEM simulation was needed to compute the actual stress experienced by each FBG, since it was clearly not possible to install SGs and FBGs exactly in the same locations.

2.1 *Static tests on the tail beam*

The front frame of the tail beam was clamped on a test stand with a dedicated support, manufactured in welded steel with a much higher stiffness than the test sample. A static load was applied through a set of calibrated weights hanging from a support clamped at the connection interface for the V-tail empennages.
The test stand allowed to apply a bending load (weight applied on the fuselage centerline) or a combination of bending and torsion loads (weight applied offset from the fuselage centerline).
The static test stand for the tail beam is shown in Figure 4.
The application of a static load allowed to compare the deformation predicted by the FEM analysis to that measured by the strain gages and FBGs. The results of this phase are shown in Figure 5.

Fig. 4. Experimental setup for the static load tests on the tail beam

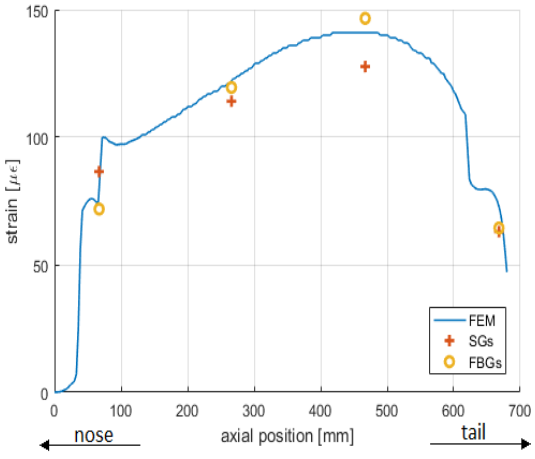

Fig. 5. Comparison of FBG measurements, SG measurements, and FEM analysis for the tail beam under a 30N bending load applied at the empennages interface. The axial position coordinate refers to the distance from the clamping constraint.

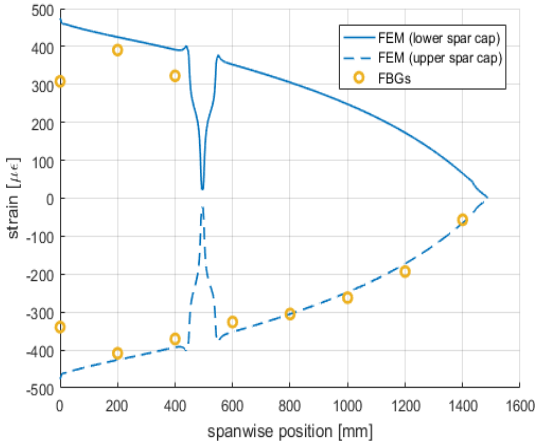

Fig. 6. Comparison of FBG measurements and FEM analysis for wing sections 3 and 4, under a 20N bending load applied at the tip of section 4. The spanwise position coordinate refers to the distance from the aircraft centreline.

Figure 5 shows the comparison between the different strain estimates in the case of a bending load applied at the connection of the empennages. The FEM analysis shows estimates a regular strain distribution for the middle section of the tail beam. The irregular behavior of the forward section (near the constraint) and the tip section is due to the abrupt variations in geometry and boundary conditions. Both the strain gages and FBGs are mostly matching with the FEM estimate, except for the SG at the 467mm position, which has a 13% discrepancy with both the FEM and FBGs. This is due to a defective bonding of the strain gage, failing to transfer correctly loads and deformations.

2.1 *Static tests on the wing*

A similar static test was carried out for the instrumented wing sections. A support was built to clamp the center section of the wing to the test stand, with a stiff interface geometrically similar to the actual wing-fuselage connection. Loads were applied near the wing tip with the same calibrated weights of the fuselage static tests. The wing was installed on the test stand upside down, in order for the calibrated load to simulate lift. Figure 7 shows the test stand for the wing, while Figure 6 shows the results of this experiment, comparing FEM and FBGs; no strain gages were installed on the wing.
The FEM analysis estimates the strain distribution on the top and bottom spar caps, highlighting the discontinuities near the junctions between adjacent sections (see the red curves of Figure 6 near the 500mm position, corresponding to the joint between wing section 3 and 4). The FBG measures match the FEM estimates, except for the sensors lying on the fuselage centreline. These are within the clamping system, and here the FEM model may be inaccurate due to the assumption of a perfectly stiff clamp. Additionally, the sensors are not able to capture the discontinuity at 500mm, since the junction lies halfway between two sensors; this placement was necessary for allowing the space required by the optical connector for the disassembly of the wing. By comparing Figures 5 and YY, the wing is an order of magnitude more flexible than the tail beam. This simplifies the acquisition of the strain values, since those on the tail are much smaller and closer to the sensor resolution.

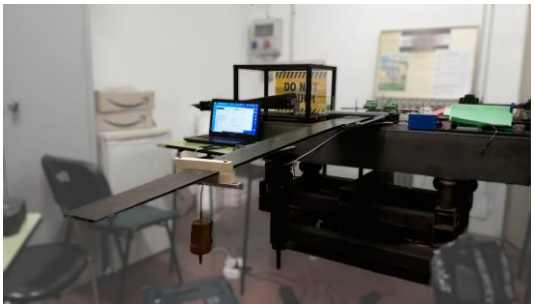

Fig. 7. Experimental setup for the static load tests on the wing

2. Flight tests results

In order to determine the quality of data measured in an on-field application of the proposed technology, we performed a campaign of flight tests. Those allowed to determine the sensitivity of the system to actual flight loads, as well as the effect of noise, vibrations and thermal gradients on measured data.
The schedule for the flight test only allowed to assess the sensors installed on the tail beam, as the sensored wing was still undergoing the manufacture and assembly process.
During the fight tests we acquired the measurements from the 16 sensors installed on the tail beam and the accelerations and angular rates from the Inertial Measurement Unit (IMU).
Figure 8 shows the accelerations and angular rates during the test; the acquisition covers two flights of the UAV, for a total duration of about 50 minutes. The measures are filtered to hide the vibrations from the propulsion system and show the accelerations due to the maneuvers.

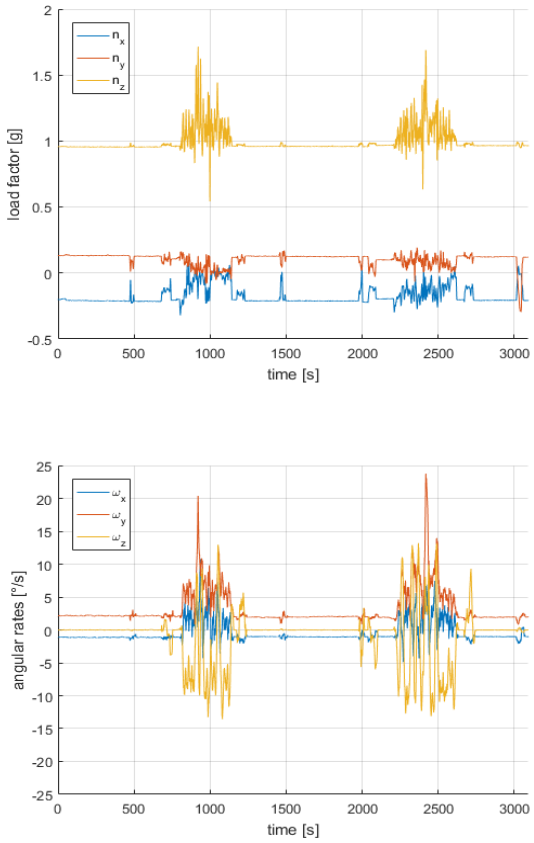

Fig. 8. Load factor (top) and angular rates (bottom) experienced by the UAV during the flight test (from integrated six-axis MEMS accelerometer and gyroscope)

Figure 9 shows the four channels of the interrogator. A moving average filter with a window size of 100ms was applied to the raw data in order to reduce noise and filter out the vibration from the motor and propeller. Data of Figure 9 are not temperature compensated. Comparing the measured strains with the load factor time history, we observe a significant drift in the strain on all channels when the aircraft is on ground (n=1). This is due to the temperature variation when the carbon structure is exposed to direct sunlight. As a first preliminary attempt for thermal compensation, for each sensor position on the longitudinal axis of the fuselage, the average of the lower sensors was subtracted to the average of the upper sensors. Since the structure is subject to a mostly bending load, if temperature is uniform, thermal expansion will be responsible for an equal deformation of the upper and lower skins, while mechanical loads will result in an antisymmetric strain component.

The estimated mechanical component of the strain is shown in Figure 10. The tail beam of the UAV employed for this experimental campaign is very stiff and produces small displacements under flight loads. Consequently, the mechanical component of strain is comparable to thermal expansion resulting from environmental conditions (i.e. temperature variations with altitude, exposition to direct sunlight, etc.). The upcoming flight test with the instrumented wing is expected to provide better results regarding the disturbance of thermal expansion. Additionally, the wing is equipped with an unloaded FBG as a temperature sensor for thermal compensation.

2. Conclusions

An Optical Structural Health Monitoring System based on Fiber Bragg Grating sensors was developed and assessed on a UAV platform, with both static and flight tests. The system performed as expected and was able to measure in the strain of structural components under actual flight loads. The experimental campaign proved that FBG sensors allow the integration of a Structural Health Monitoring system with minimal invasivity on an airborne platform. Additionally, we concluded that thermal compensation is necessary to achieve the required accuracy for aerodynamic load estimation. Work currently in progress includes the development of postprocessing algorithms in order to determine aerodynamic loads on the flight control actuators, as well as the upgrade of the system to stream telemetry data in real time.

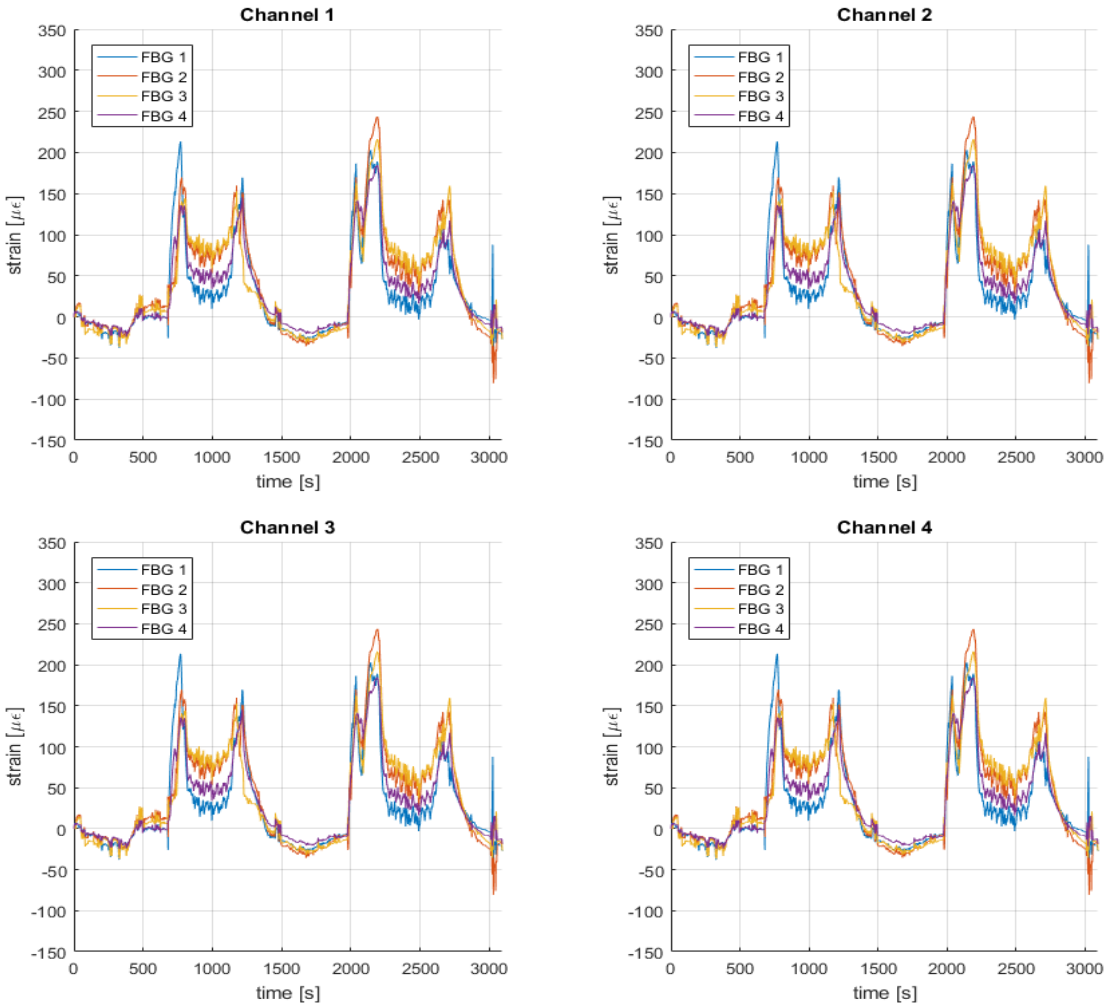

Fig. 9. Strain sensed by the tail beam FBGs

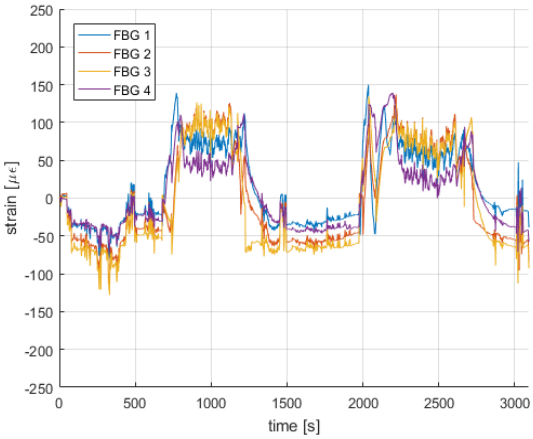

Fig. 10. Estimated mechanical component of the strain.

Acknowledgement

This work was supported by the Photonext interdepartmental center at Politecnico di Torino. The authors wish to thank the LINKS laboratory and the ICARUS students team for their invaluable assistance to the experimental activities presented in this paper.

Appendix A. Hinge Load Reconstruction

This paragraph describes an example of a simplified algorithm for hinge moment reconstruction. A more accurate study, involving a combination of FEM, Computational Fluid Dynamics (CFD) and Machine Learning (ML) is under development and will be the subject for a future paper.

The lift produced by the V-tail can be expressed as:

$$\Delta L_t = \frac{1}{2}\rho V_\infty^2 S_t \Delta C_{l,t} = \frac{1}{2}\rho V_\infty^2 \frac{c_V}{c_t} S_t c_{l\alpha,t} \delta_V \#(1)$$

And assuming that the additional lift is applied at 25% of the chord of the control surface, the resulting hinge moment can be computed as:

$$M_V = \frac{1}{4}\Delta L_t c_V \#(2)$$

The vertical load applied to the tail beam is:

$$F = 2L_t \cos\Gamma \#(3)$$

Where Γ is the dihedral angle of the V-tail. Hence, the hinge moment with this simplified model is directly proportional to the load on the tail beam:

$$M_V = \frac{1}{4} c_V \frac{\Delta \mathrm{F}}{2\cos\Gamma} \#(4)$$

This simplified algorithm allows to estimate the actuator load from the force experienced by the tail beam, which can be derived from the measured strains. Of course, a more accurate strategy will be required to be employed in a model based fault detection algorithm.

References

Anderson, R.J. and S.R. Aylward (1993). Lab Testing of Neural Networks for Improved Aircraft Onboard-Diagnostics on Flight-Ready Hardware. *Annual Reliability and Maintainability Symposium*.

Berri, P.C., M.D.L. Dalla Vedova and L. Mainini (2018). Diagnostics of Actuation System Faults from Dynamic Data, *6th European Conference on Computational Mechanics (ECCM 6).*

Berri, P.C., M.D.L. Dalla Vedova and L. Mainini (2019a). Real-time Fault Detection and Prognostics for Aircraft Actuation Systems, *AIAA SciTech Forum,* AIAA 2019-2210.

Berri, P.C., M.D.L. Dalla Vedova, P. Maggiore and T. Scolpito (2019b). Feasibility study of FBG-based sensors for prognostics in aerospace applications. *Journal of Physics: Conference Series 1249,* 012015.

Dalla Vedova, M.D.L., P.C. Berri and S. Re (2019). Novel Metaheuristic Bio-Inspired Algorithms for Prognostics of Onboard Electromechanical Actuators. *International Journal of Mechanics and Control 19(2),* 95-101.

De Martin, A., M. Sorli and G. Jacazio (2019). Integrated Health Monitoring for Robust Actuation System of UAV Prymary Flight Controls. *International Journal of Mechanics and Control 20(2).*

Hasan, A. and T.A. Johansen (2018). Model-Based Actuator Fault Diagnosis in Multirotor UAVs. *International Conference on Unmanned Aircraft Systems.*

Mainini, L. and K.E. Willcox (2017b) Data to Decisions: Real-Time Structural Assessment from Sparse Measurements Affected by Uncertainty. *Computers & Structures 182,* 296-312.

Mihailov, S.J. (2012). Fiber Bragg grating sensors for harsh environments. *Sensors 12(2)*, 1898-1918.

Mihailov, S.J., D. Grobnic, C. Hnatovsky, R.B. Walker, P. Lu, D. Coulas and H. Ding (2017). Extreme Environment Sensing Using Femtosecond Laser-Inscribed Fiber Bragg Gratings. *MDPI Sensors 17(12),* 2909.

Santos, J.L. and F. Farahi (2018). *Handbook of Optical Sensors*, CRC Press.

Tanaka, N., Y. Okabe and N. Takeda (2003). Temperature-compensated strain measurement using Fiber Bragg Gratings sensors embedded in composite laminates. *Smart Materials & Structures 12(6),* 940–946.

Willcox, K.E. and L. Mainini (2017a). Sensor placement strategy to inform decisions. *18th AIAA/ISSMO Multidisciplinary Analysis and Optimization Conference.*